Banff International Research Station
for Mathematical Innovation and Discovery

Recent Progress in Detection and Prediction of Epilepsy
Saturday October 15th 2022 (3:30 p.m.)

Cross-frequency coupling studies of intracranial EEG data of epilepsy patients using time-frequency distributions

Daniel Girvitz[1]

Supervisor: Dr. Kris Vasudevan[1]
Supervisor: Dr. Elena Braverman[1]

[1]Department of Mathematics and Statistics, University of Calgary

NSERC CRSNG

Hotchkiss Brain Institute

University of Calgary

In memoriam

Dr. Kris Vasudevan
March 2nd 1944 – August 22nd 2022

Dedicated to an inspiring mentor, caring supervisor – and just a great friend,

with whom I am proud to have worked,

and proud to have made proud.

Contents

1. Motivation; definitions of CFC, PAC
2. Essentials we need; metric definitions
3. Methods for Detecting CFC
4. Methods for Detecting CFC: MVL, MI, GLM
5. Traditional method vs. time-frequency method
6. Problems with the TF method
7. Cohen's class of TF distributions
8. Reduced Rihaczek distribution & method
9. Real Data Examples: MVL method, plus analysis & interpretation
10. Conclusions
11. Sources

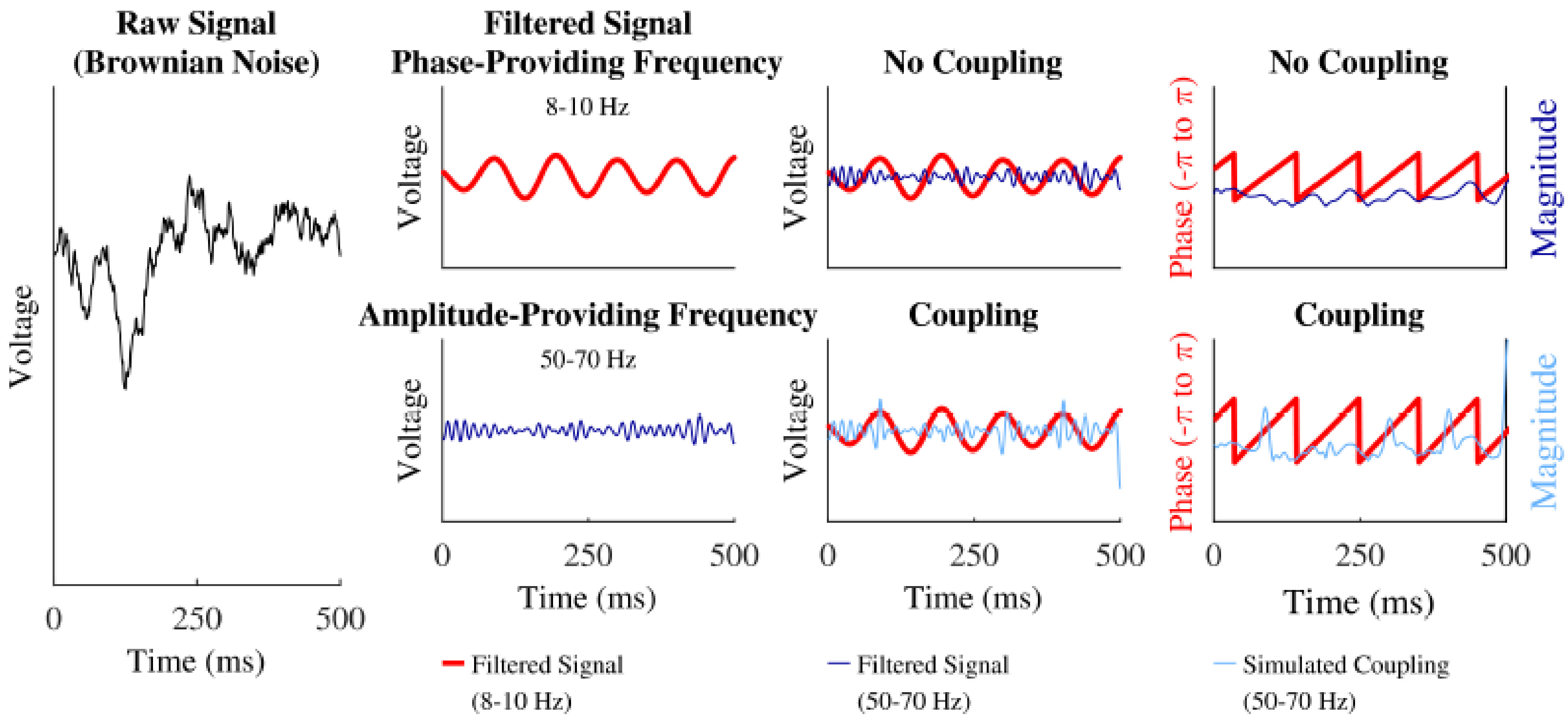

Motivation; definitions of CFC, PAC

Taken from *Hülsemann M.J., Naumann E. and Rasch B.* — Quantification of Phase-Amplitude Coupling in Neuronal Oscillations: Comparison of Phase-Locking Value, Mean Vector Length, Modulation Index, and Generalized-Linear-Modeling-Cross-Frequency-Coupling. — // Front. Neurosci. — 2019. — Vol. 13 — P. 573.

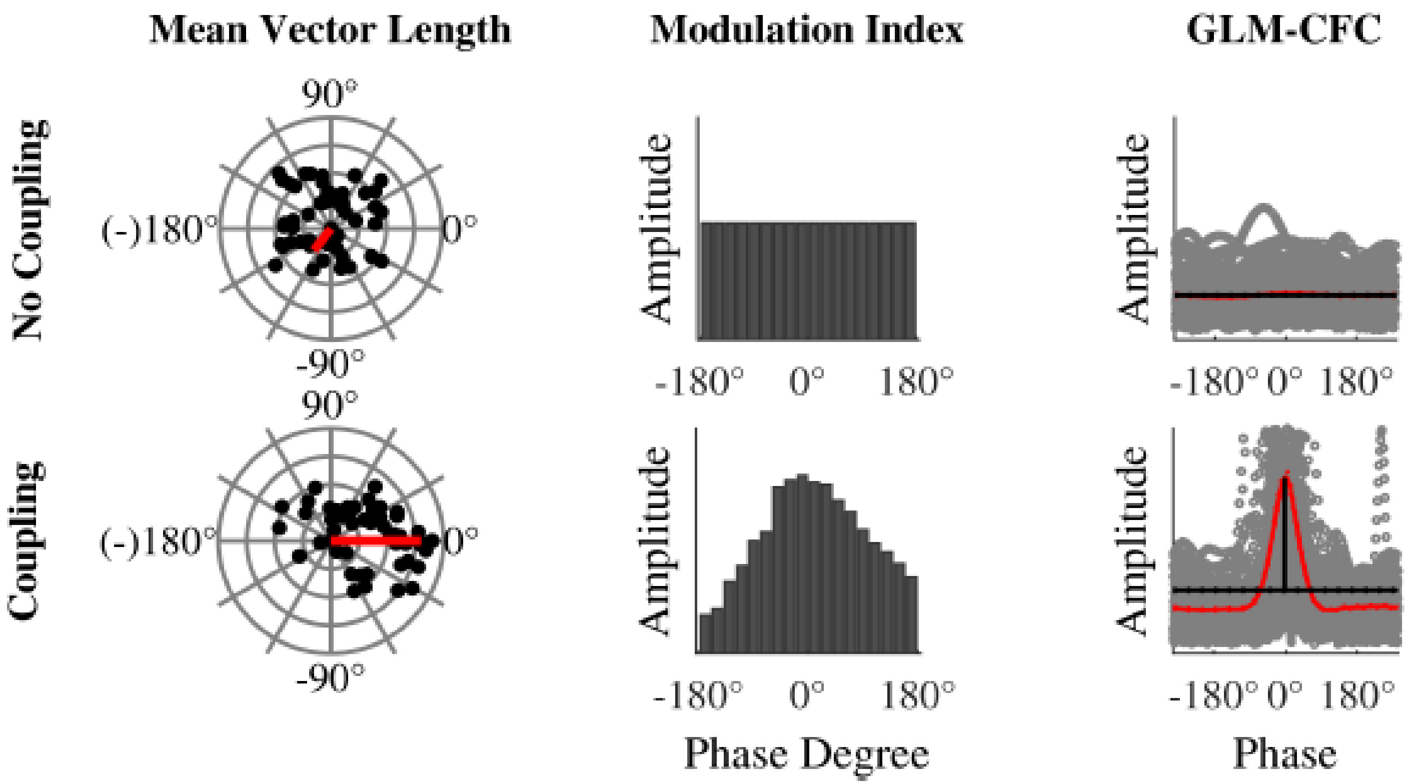

Essentials we need (phase & amplitude estimates); metric definitions i.e. how to quantify PAC?

Taken from *Hülsemann M.J., Naumann E. and Rasch B.* — Quantification of Phase-Amplitude Coupling in Neuronal Oscillations: Comparison of Phase-Locking Value, Mean Vector Length, Modulation Index, and Generalized-Linear-Modeling-Cross-Frequency-Coupling. — // Front. Neurosci. — 2019. — Vol. 13 — P. 573.

Methods for Detecting CFC

1. **Mean Vector Length (MVL)** -- Canolty et al (2006)
2. **Modulation Index (MI)** -- Canolty et al (2006), Tort et al (2010)
3. **GLM-CFC** -- Penny et al (2008), Voytek et al (2013), Mark & Kramer (2013), Nadalin et al (2019)

4. Phase-locking Value (PLV) -- Mormann et al (2005), Lachaux et al (1999), Vanhatalo et al (2004)
5. Correlation Coefficient -- Penny et al (2008)
6. Envelope-to-signal Correlation -- Bruns and Eckhorn (2004)
7. Analysis of amplitude spectra – Cohen (2008)
8. Coherence between amplitude and signal -- Colgin et al (2009)
9. Coherence between the time course of power and signal -- Osipova et al (2008)
10. Eigendecomposition of multichannel covariance matrices -- Cohen (2017)

Methods for detecting CFC -- MVL

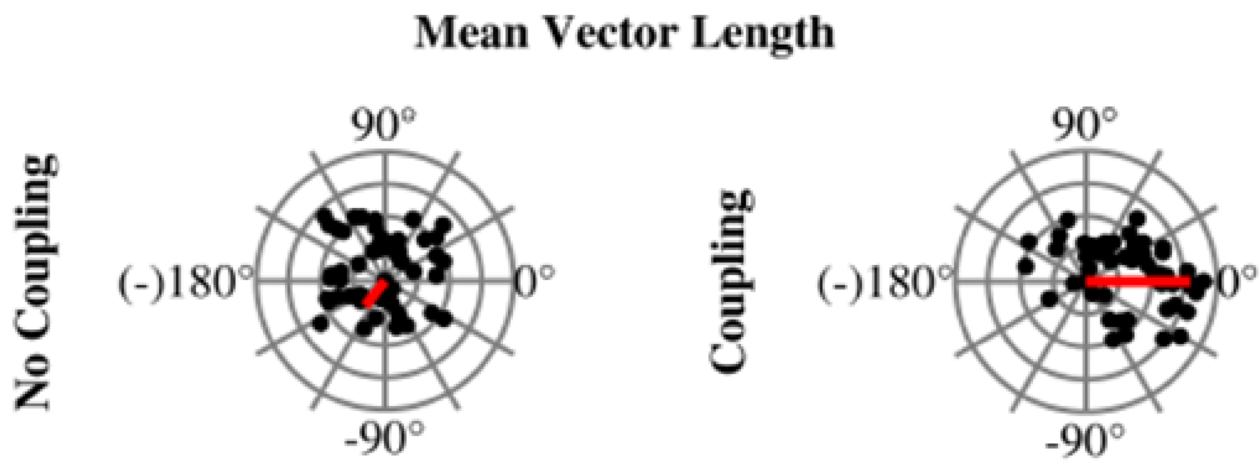

$$MVL = \frac{\sum_{n=1}^{N} \left\| A_{f_A}[n] e^{j\varphi_{f_p}[n]} \right\|}{N}$$

Methods for detecting CFC -- MI

$$P(j) = \frac{\langle A_{f_A} \rangle_{\varphi_p}(j)}{\sum_{k=1}^{K} \langle A_{f_A} \rangle_{\varphi_{f_p}}(k)} \qquad MI = \left[\frac{D_{KL}(P,U)}{\log(N)}\right]$$

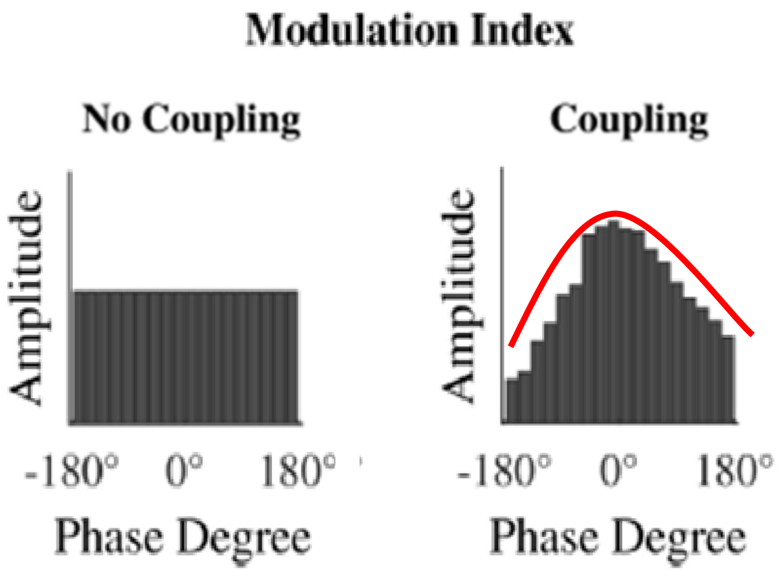

The KL Distance quantifies the amplitude (over binned phases) distribution's deviation from the Uniform distribution.

1. $\langle A_{f_A} \rangle_{\varphi_{f_p}}$ -- mean of instantaneous amplitude values over binned phases, with bins j
2. $P(j) = \frac{\langle A_{f_A} \rangle_{\varphi_p}(j)}{\sum_{k=1}^{K} \langle A_{f_A} \rangle_{\varphi_{f_p}}(k)}$ -- amplitude distribution, where $P(j) \geq 0 \ \forall \ j$ and $\sum_{j=1}^{J} P(j) = 1$
3. $D_{KL}(P,Q) = \sum_{j=1}^{J} P(j) \log\left[\frac{P(j)}{Q(j)}\right]$ -- Kullback-Leibler (KL) distance, where $D_{KL}(P,Q) \geq 0$, and $D_{KL}(P,Q) = 0 \iff P = Q$
4. $H(P) = -\sum_{j=1}^{J} P(j) \log[P(j)]$ -- Shannon Entropy
5. $D_{KL}(P,U) = \log(N) - H(P)$ -- relationship b/ween Shannon entropy and KL distance
6. $MI = \left[\frac{D_{KL}(P,U)}{\log(N)}\right] = \left[\frac{D_{KL}(P,U)}{D_{KL}(P,U)+H(P)}\right]$ -- definition of MI

Methods for detecting CFC -- GLM

Proposed by Kramer & Eden (2013); expanded to include other models by Nadalin et al (2019)

The $\boldsymbol{\varphi_{low}}$ model -- relates A_{high}, the response variable, to a linear combination of φ_{low}, the predictor variable, expressed in a spline basis.

$$A_{high}|\varphi_{low} \sim Gamma[\mu, v]$$

- Gamma distribution is chosen because it ensures real, positive amplitude values: The Gamma distribution is common for data for which the sd increases linearly with the mean
- μ is the mean parameter
- v is the shape parameter

$$\log \mu = \sum_{k=1}^{K} \beta_k f_k(\varphi_{low})$$

- Log-link functions are common are GLMs using Gamma distributions, and leads to models where predictors have multiplicative effects on the response
- β_k are underdetermined coefficients
- Functions $\{f_1, \ldots, f_n\}$ correspond to spline basis functions, with n control points equally spaced between 0 and 2π, used to approximate φ_{low}
  - Spline basis functions sum to 1
  - n set to 10 because experiments have shown it is a sound choice to identify PAC with one or two broad peaks; determination of n is performed using the AIC: $AIC = \Delta + 2n$
  - Tension parameter of 0.5 to control smoothness of splines

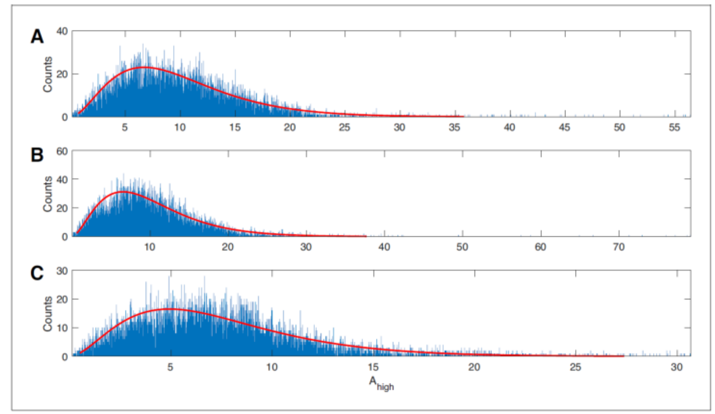

Taken from Nadalin et al – A statistical framework to assess cross-frequency coupling while accounting for confounding analysis effects. – // Elife. – 2019 Oct 16. – doi:10.7554/eLife.44287

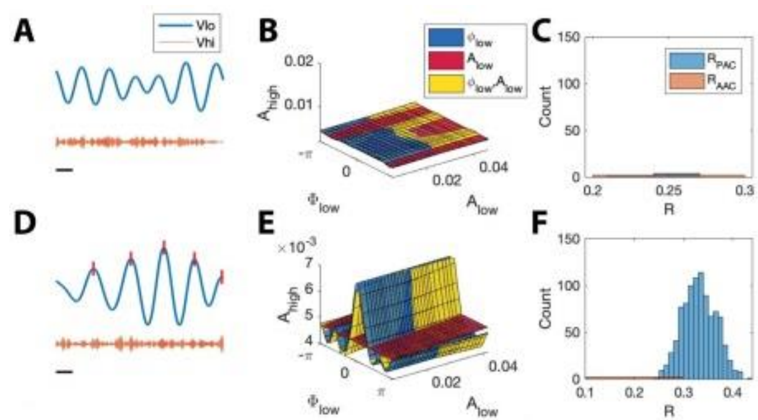

Taken from Nadalin et al – A statistical framework to assess cross-frequency coupling while accounting for confounding analysis effects. – // Elife. – 2019 Oct 16. – doi:10.7554/eLife.44287

Note: the use of the basis/cardinal spline functions move the model into the larger class of Generalized Additive Models (GAMs)

Methods for detecting CFC -- GLM

1. **The $\boldsymbol{\varphi_{low}}$ model** -- relates A_{high}, the response variable, to a linear combination of φ_{low}, the predictor variable, expressed in a spline basis
   - $A_{high}|\varphi_{low} \sim Gamma[\mu, v]$ -- conditional distribution of A_{high} given φ_{low}
   - $\log \mu = \sum_{k=1}^{K} \beta_k f_k(\varphi_{low})$

2. **The $\boldsymbol{A_{low}}$ model** -- relates the high frequency amplitude to the low frequency amplitude
   - $A_{high}|A_{low} \sim Gamma[\mu, v]$ -- conditional distribution of A_{high} given A_{low}
   - $\log \mu = \beta_1 + \beta_2 A_{low}$

3. **The $\boldsymbol{A_{low}, \varphi_{low}}$ model** -- extends the φ_{low} model by including three additional predictors
   - $A_{high}|\varphi_{low}, A_{low} \sim Gamma[\mu, v]$ -- conditional distribution of A_{high} given φ_{low} and A_{low}
   - $\log \mu = \sum_{k=1}^{K} \beta_k f_k(\varphi_{low}) + \beta_{n+1} A_{low} + \beta_{n+2} A_{low} \sin(\varphi_{low}) + \beta_{n+3} A_{low} \cos(\varphi_{low})$

4. **Evaluate the model in 3D using MATLAB function ‘glmfit’**
   i. Create surface $S_{A_{low},\varphi_{low}}$, which fits the A_{low}, φ_{low} model in 3D $(A_{low}, \varphi_{low}, A_{high})$ space
   ii. Create surface $S_{A_{low}}$, which fits the A_{low} model in 3D $(A_{low}, \varphi_{low}, A_{high})$ space
   iii. Create surface $S_{\varphi_{low}}$, which fits the φ_{low} model in 3D $(A_{low}, \varphi_{low}, A_{high})$ space

5. **rPAC statistic** -- measures the effect ϕ_{low} on A_{low}, while accounting for fluctuations in A_{low}
   - $rPAC = \max\left[abs\left[\frac{1-S_{A_{low}}}{S_{A_{low},\varphi_{low}}}\right]\right]$ -- maximum absolute fractional difference b/ween resulting surfaces $S_{A_{low}}$ and $S_{A_{low},\varphi_{low}}$

Note: ‘glmfit’ uses the Fischer scoring/Iteratively reweighted least squares algorithm

Traditional (Hilbert-transform) method vs. time-frequency method

Hilbert-transform method

$$\mathcal{H}\{f(\tau)\}(t) = f(t) * \frac{1}{\pi \mathrm{t}} = \frac{1}{\pi} \int_{-\infty}^{\infty} \frac{f(\tau)}{t-\tau} d\tau$$

The Hilbert transform is an integral transform, procured through the convolution operation.

The method involves (1) filtering the signal before (2) converting the filtered low- and high-frequency components into their analytic representations, from which one can (3) procure the phase and amplitude estimates through the arctangent and absolute value operations respectively.

phase_low = arctangent(hilbert(V_low))

amp_high = abs(hilbert(V_high))

Time-frequency method

$$E = \iint_D P(t, \omega)\, d\omega\, dt$$

Total energy of the signal as a function of its tf distribution.

The time frequency method involves the use of a function, called the distribution, with variables time t and frequency ω, which represents the energy or intensity per unit time per unit frequency, namely $P(t, \omega)$. The signal's total energy is given by the integration of the distribution across its t-f domain.

Like with the Hilbert-transform method, both phase and amplitude are extracted using the arctangent and absolute value operations.

Hilbert-transform method

1. **Choose signal $\boldsymbol{x_{raw}[n]}$ and filter it to give**
   - $x_{f_p}[n] = LPF\{x_{raw}[n]\}$ -- phase-giving signal
   - $x_{f_A}[n] = HPF\{x_{raw}[n]\}$ -- amplitude-giving signal

2. **Convert signals $\boldsymbol{x_{f_p}[n]}$ and $\boldsymbol{x_{f_A}[n]}$ to analytic form using the Hilbert transform**
   - $\left[x_{f_p}[n]\right]_a = x_{f_p}[n] + i\mathcal{H}\left\{x_{f_p}[n]\right\}$ -- analytic signal representation of $x_{f_p}[n]$
   - $\left[x_{f_A}[n]\right]_a = x_{f_A}[n] + i\mathcal{H}\left\{x_{f_A}[n]\right\}$ -- analytic signal representation of $x_{f_A}[n]$

3. **Procure instantaneous phase & amplitude values**
   - $\varphi_{f_p}[n] = \arctan\left[x_{f_p}[n]\right]_a$ -- instantaneous phase values
   - $A_{f_A}[n] = \left\|\left[x_{f_A}[n]\right]_a\right\|$ -- instantaneous amplitude values

Note: [n] refers to sample n in an N-sized signal, which MATLAB treats as a vector

Problems with the TF method

Let $y(t) = \cos(2\pi f_1 t) + \cos(2\pi f_2 t) \begin{cases} f_1 = 10,\ f_2 = 15,\ 0s \le t < 1s \\ f_1 = 20,\ f_2 = 25,\ 1s \le t < 2s \\ f_1 = 30,\ f_2 = 35,\ 2s \le t < 3s \\ f_1 = 40,\ f_2 = 45,\ 3s \le t < 4s \end{cases}$

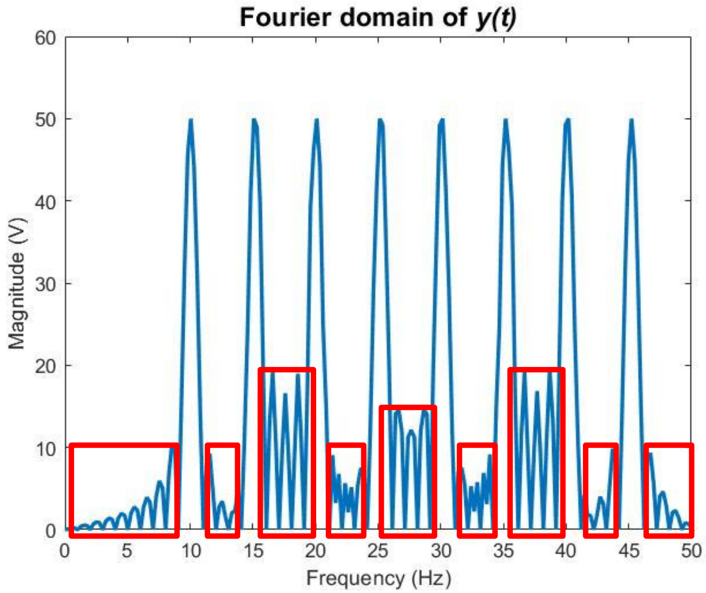

Traditional Fourier transform methods fail to account for changing frequencies.

Also, **spectral leakage** has been introduced.

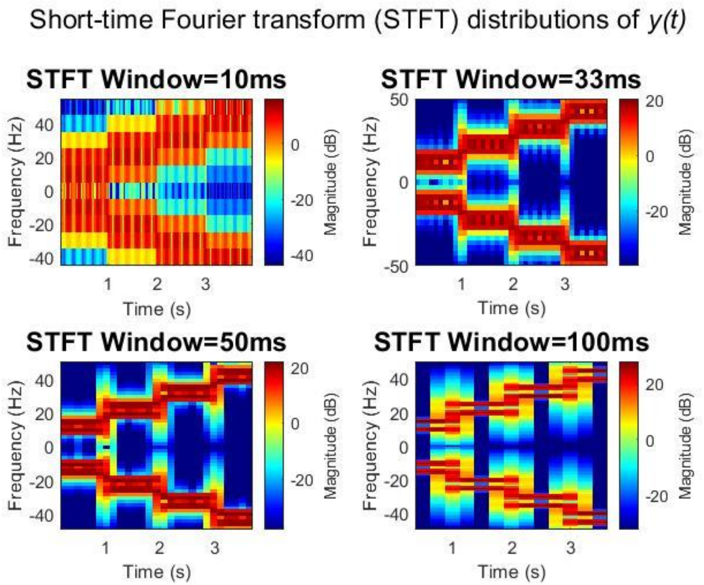

Better resolution in the time domain results in worse resolution in the frequency domain and vice-versa -- i.e. the Heisenberg uncertainty principle.

Cohen's class of TF distributions

Are all generalizations of

$$P(t,\omega) = \frac{1}{4\pi^2}\iiint e^{-j\theta t - j\tau\omega + j\theta u}\boxed{\boldsymbol{\phi(\theta,\tau)}}\, s^*\left(u-\frac{1}{2}\tau\right) s\left(u+\frac{1}{2}\tau\right) du\, d\tau\, d\theta$$

where $\phi(\theta,\tau)$ is an arbitrary function called the kernel function originally by Claasen and Mecklenbrauker. Choosing different kernel functions results in different distributions, each with their own properties.

For the Wigner, Rihaczek, and Page distributions, these are their respective kernel functions:
$\boldsymbol{\phi(\theta,\tau) = 1, e^{j\theta\tau/2}, e^{j\theta|\tau|/2}}$
(kernel #1 – next slide)

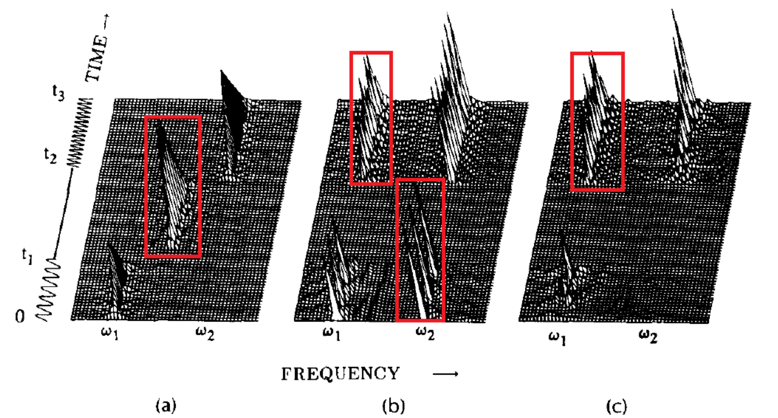

Fig. 1. (a) Wigner, (b) Rihaczek, and (c) Page distributions for the signal illustrated at left. The signal is turned on at time zero with constant frequency ω_1 and turned off at time t_1, turned on again at time t_2 with frequency ω_2 and turned off at time t_3. All three distributions display energy density where one does not expect any. The positive parts of the distributions are plotted. For the Rihaczek distribution we have plotted the real part, which is also a distribution.

Taken from *Cohen L.* — Time-frequency distributions-a review. — // Proceedings of the IEEE. — 1989. — Vol. 77, no. 7. — P. 941–981.

Reduced Interference (RID) - Rihaczek time-frequency distribution

$$C(t,f) = \iint \boxed{\exp\left(-\frac{(\theta\tau)^2}{\sigma}\right)} \boxed{\exp\left(j\frac{\theta\tau}{\sigma}\right)} \boxed{A(\theta,\tau)} e^{-j(\theta t + 2\pi f\tau)}\, d\tau d\theta$$

Where $\exp\left(-\frac{(\theta\tau)^2}{\sigma}\right)$ is the Choi-Williams kernel

Where $\exp\left(j\frac{\theta\tau}{\sigma}\right)$ is the kernel function for the reduced-Rihaczek distribution (aforementioned kernel #1)

- reduces the effect of the cross-terms and localizes the energy and phase estimates

Where $A(\theta,\tau) = \int x\left(u+\frac{\tau}{2}\right) x^*\left(u-\frac{\tau}{2}\right) e^{i\theta u}\, du$ is the ambiguity function

- Both kernel functions can be thought of as two-dimensional lowpass filters that act on the ambiguity function that captures the time-varying autocorrelation of the signal
- The ambiguity function itself pulls interference terms into central locations, thereby minimizing their influence

RID-Rihaczek tfd method

1. **Choose signal $\boldsymbol{x_{raw}[n]}$**

2. **Compute Reduced-Rihaczek TFD matrix using MATLAB function: rid_rihaczek4(x,Fs)**
   - Where argument x $\equiv x_{raw}[n]$
   - Where argument Fs is the sampling frequency
   - Return value is matrix TFD with size =(rows)x(columns)=(Fs/2)x(N)
     - Fs/2 refers to the Nyquist limit: Frequencies above Fs/2 will show traits of aliasing and are therefore unusable

3. **Remove 1st row of TFD because it represents the 0Hz component: essentially, a constant voltage source, like a Duracell battery**

4. **Extract two rows**
   - TFD_{low}
   - $TFD_{high} = \|A_{f_A}[n]\|^2$ -- by virtue of the theory behind the Reduced-Rihaczek tfd

5. **Procure instantaneous phase & amplitude values**
   - $\varphi_{f_p}[n] = \arctan[TFD_{low}]$ -- instantaneous phase values
   - $A_{f_A}[n] = \sqrt{\|A_{f_A}[n]\|^2} = \sqrt{\|TFD_{high}\|}$ -- instantaneous amplitude values

Note: [n] refers to sample n in an N-sized signal, which MATLAB treats as a vector

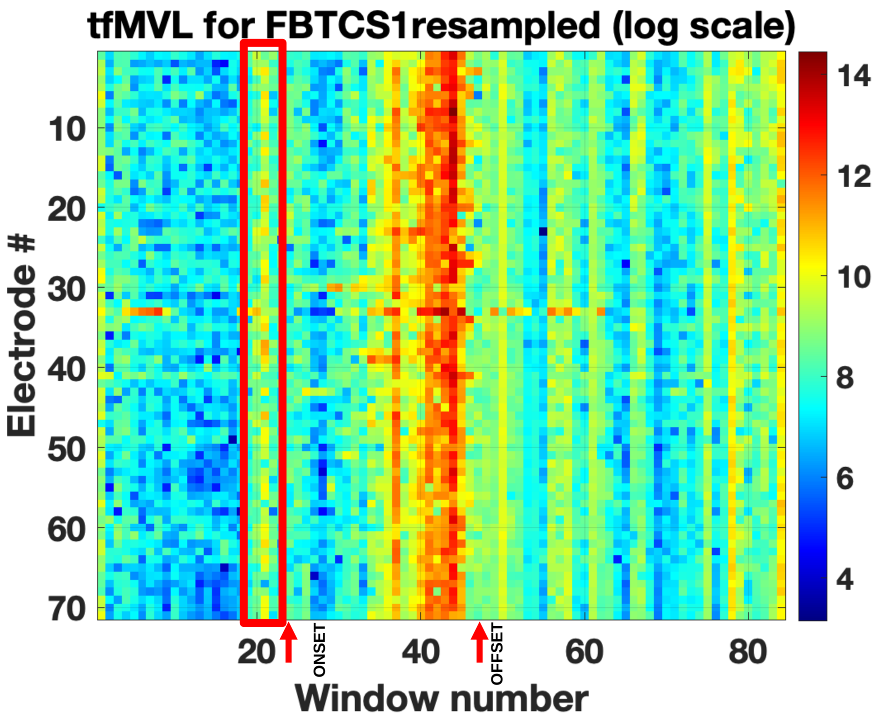

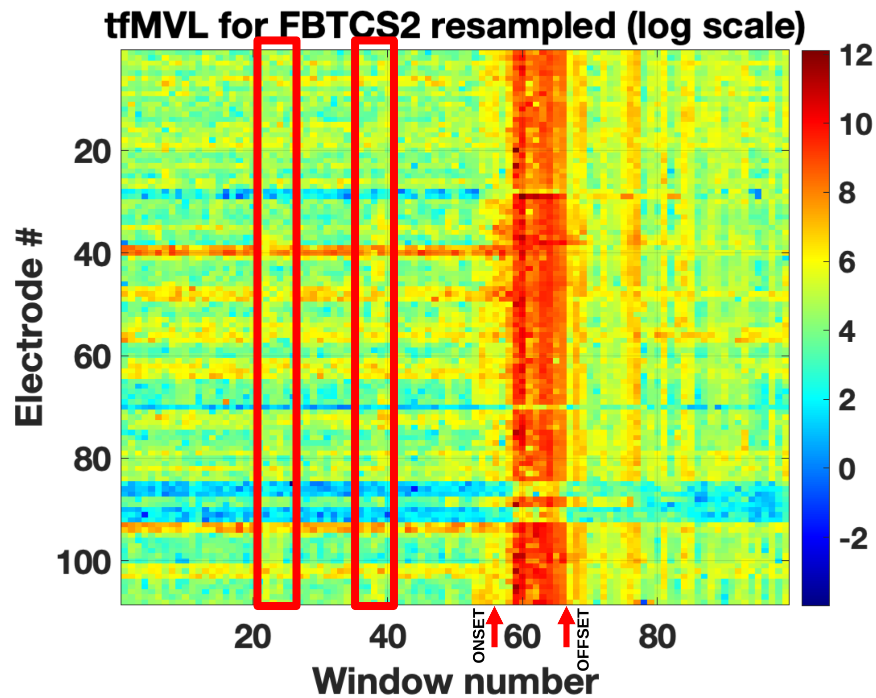

Real Data Examples: MVL method, plus analysis & interpretation

Each pixel refers to intra-electrode coupling (i=j for a given window).

FBTCS1: there is a clear CFC signature preceding the physical onset marker by 20 seconds

FBTCS2: there are two different window locations preceding the onset where the CFC signature is evident

Note: Having tested both a linear- and log-scale, we found the log-scale allows us to discern finer features in the data

Conclusions

- The tfMVL method has clearly uncovered evidence of electrophysiological signatures in two iEEG datasets – more are required to confirm our findings
- The tf method is a viable alternative to the Hilbert-transform method

Thank you!

UNIVERSITY OF CALGARY
HOTCHKISS BRAIN INSTITUTE
NSERC CRSNG

Sources

- Aviyente & Mutlu -- A Time-Frequency-Based Approach to Phase and Phase Synchrony Estimation (2011)
- Buzsáki, G., Rhythms of the brain, Oxford University Press (2006)
- Canolty et al -- High Gamma Power Is Phase-Locked to Theta Oscillations in Human Neocortex (2006)
- Hulsemann -- Quantification of PAC in Neuronal Oscillations (Comparison of PLV, MVL, MI, GLM-CFC) (2019)
- Kramer & Eden -- Assessment of CFC with confidence using GLMs (2013)
- Munia & Aviyente -- Time-Frequency Based Phase-Amplitude Coupling Measure For Neuronal Oscillations (2019)
- Nadalin et al -- A statistical framework to assess cross-frequency coupling while accounting for confounding analysis effects (2019)
- Tort et at -- Measuring Phase-Amplitude Coupling Between Neuronal Oscillations of Different Frequencies (2010)

Note: Esoteric facts and figures cited at location, while more prominent information is analyzed from several sources, all listed